Research Square

Preprints are preliminary reports that have not undergone peer review. They should not be considered conclusive, used to inform clinical practice, or referenced by the media as validated information.

Improving Corrosion and Wear Performance for Ti-6Al-4V in Simulated Body Fluid via Plasma Sputtering

Noor Hashim Abd Almunaf

noor.abd@atu.edu.iq

Al-Furat Al-Awsat Technical University (ATU)

Hawraa Fadhel

Technical Engineering College/ Najaf, Al-Furat Al-Awsat Technical University (ATU)

Furqan Wahhab Abdulsads

Al-Furat Al-Awsat Technical University (ATU)

Thamar Ali Almussawy

Al-Qadisiya Polytechnic College, Al-Furat Al-Awsat Technical University(ATU)

Research Article

Keywords: wear performance, Corrosion behavior, Plasma Sputtering, Ti-6Al-4V alloy

Posted Date: October 15th, 2026

DOI: https://doi.org/10.21203/rs.3.rs-11112590/v1

License: This work is licensed under a Creative Commons Attribution 4.0 International License. Read Full License

Additional Declarations: No competing interests reported.

Improving Corrosion and Wear Performance for Ti-6Al-4V in Simulated Body Fluid via Plasma Sputtering

Noor Hashim Abd Almunaf [1], Hawraa Fadhel [2], Furqan Wahhab Abdulsads[3],Thamar Ali Almussawy[4]

[1]Department of Building and Construction Technical Engineering, College of Najaf, Al-Furat Al-Awsat Technical University (ATU), Najaf, Iraq.

[2] Department of Technical Power Mechanics, Technical Engineering College / Najaf, Al-Furat Al-Awsat Technical University (ATU), Najaf, Iraq.

[3] Department of Communications Engineering Technologies, Faculty of Engineering Technical / Najaf, Al-Furat Al-Awsat Technical University (ATU), Najaf, Iraq.

[4] Department of Prosthetic and Orthodontic, Al-Qadisiya Polytechnic College, Al-Furat Al-Awsat Technical University (ATU), Al-Qadisiya, Iraq

E-Mail: noor.abd@atu.edu.iq

ABSTRACT

Plasma sputtering is widely used to improve the surface properties of metals. In this study, plasma sputtering was used to enhance the surface properties of Ti-6Al-4V alloy, which is commonly used in biomedical application, due to its superior strength-to-weight ratio, excellent corrosion resistance, and outstanding fatigue performance. Despite these good properties, there is an obstacle when using it in the human body, especially for knees replacements, as it has low wear resistance in aggressive surroundings. Plasma was applied in a vacuum chamber to a titanium rod for different periods (3 and 6) hours, respectively. The chemical composition of the alloy was identified before and after the sputtering process using energy-dispersive spectroscopy (EDS), and the thickness of the deposition layer and its properties were determined using a scanning electron microscope (SEM), while the phases were identified using X-ray diffraction (XRD). Tafel polarization and cyclic polarization tests were used to evaluate the general and pitting corrosion resistance respectively. Finally, a wear test was conducted in a simulated body fluid environment, where the results showed a noticeable improvement in the properties of the alloy that was treated for 6 hours. A thick layer of niobium oxide (Nb2O5) was deposited on the surface.

Keywords: wear performance, Corrosion behavior, Plasma Sputtering, Ti-6Al-4V alloy.

1. Introduction

Titanium alloys, especially α+β Ti-6Al-4V alloy, have excellent biocompatibility, good corrosion resistance, and strength-to-weight ratio that making them favored in medical applications. Compared to cobalt-based alloys and stainless steel, titanium is characterized by its ability to form a protective surface layer of titanium dioxide (TiO_2) which has high stability to the alloy surface, and its ability to protect the alloy from corrosion in body fluids [1,2]. Unfortunately, this layer has poor tribological properties, which makes it susceptible to degradation in corrosive environments, where these alloys do not fully comply with the specifications required for several application [3,4].

When this alloy is exposed to wear stresses in an aggressive medium, the protective surface layer is exposed to deterioration and fracture, which leads to the exposure of the new surface to a corrosion environment leads to the release of both vanadium and aluminum ions into the body fluid, leading to the risks of toxicity in the body [5].

To overcome this problem, the mechanical properties of the surface alloy must be improved, especially when exposed to a corrosive environment, which has been enhanced using various engineering techniques, including Physical-Vapor-Deposition, Ion-Implantation-Nitriding, Thermal-Spraying, and Plasma-Sputtering [6,7]. Furthermore, the use of plasma sputtering is particularly advantageous in biomedical applications, as it allows for the precise deposition of homogenous biocompatible coatings that can improve the corrosion resistance and wear resistance, enhancing their long-term performance in the human body, [8].

This study aims to improve the corrosion resistance and wear characteristics of biocompatible Ti-6Al-4V alloys in simulated body fluid through the plasma sputtering process to form a niobium oxide layer for different periods (3 and 6 hours) in a vacuum chamber.

2. Methodology

2.1 Materials and Methods

A titanium alloy rod provided by MC MASTER USA was used to produce a cylindrical specimen with a 16 mm diameter and 3.5 mm thickness using a DEM cutting machine. For quality assurance purposes, each sample was replicated three times to confirm the accuracy and reliability of the experimental results. The chemical composition of the alloy was examined by EDS before plasma sputtering, as shown in Figure 1:

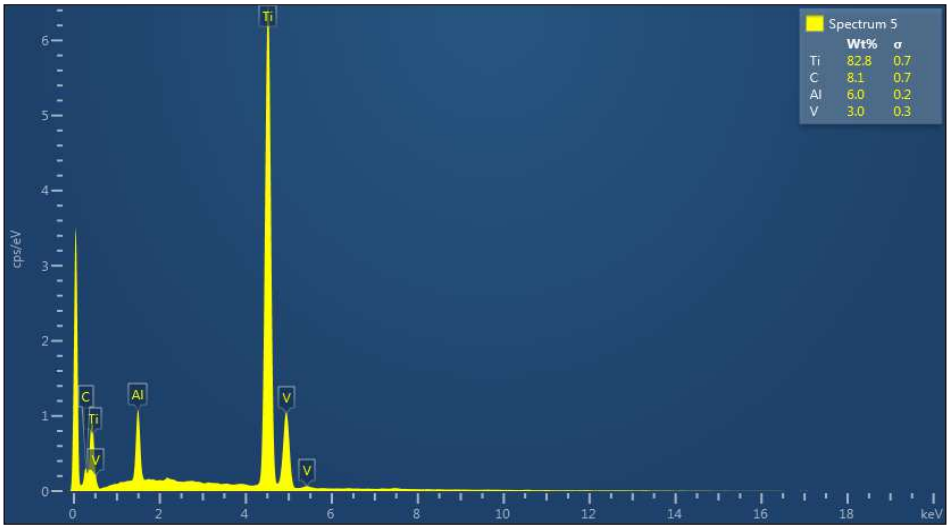

Figure-1. EDX for Ti-6Al-4V alloy before treated.

Before starting the plasma sputtering process, silicon carbide paper (120-1200 µm) was used to smooth the surface of the samples. Subsequently, the specimens were cleaned with purified water and polished using a polishing cloth with a suspended diamond solution (9,6,3, and1 µm) to obtain a shiny surface like mirrors. After that, the samples were cleaned using ultrasound with an ethanol medium for five minutes to achieve a clean surface free of any impurities. Then, the samples were dried using hot air. Kroll's reagent solution was prepared for the etching process by mixing 6 ml of water (H_2O), 3 ml of nitric acid HNO_3, and 1 ml of hydrofluoric acid (HF). These specimens were submerged in this mixture for five seconds, then rinsed with distilled water and dried by dry air, was also conducted by [9].

2.2 Plasma Sputtering for Surface Modification

Mirror-polished samples from Ti-6Al-4V alloy were processed using plasma sputtering in a DC glow discharge system for (3 and 6 hours). This system consists of a vacuum chamber that has a cylindrical shape with a diameter of 16cm and a length of 25cm ،where this system is supplied with an accessory of a high-efficiency gas discharge system to obtain low-pressure gas discharge inside the system chamber. The chamber of the system consists of two electrodes, the top one has a diameter of 7cm while the bottom one has a diameter of 12 cm, they are called the cathode and anode respectively, and the gap between them during the sputtering process is 3.3 cm [10], as shown in Figure 2.

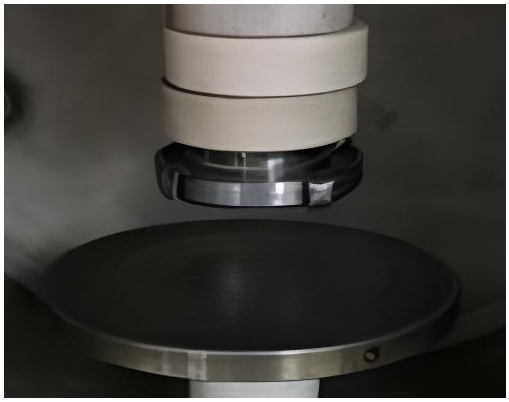

Figure-2. Electrode shape and installation before the sputtering process.

Niobium metal was installed on the cathode electrode while titanium alloy was placed on the anode electrode, the chamber was closed and evacuated from gas at a pressure of (1×10^{-5} mbar), and argon and oxygen gases were injected into the chamber at pressures of (1.1×10^{-2} and 2.4×10^{-2} mbar) respectively, where oxygen gas oxidizes niobium after being impacted by argon gas, which leads to the deposition of niobium-oxide on the surface of the titanium alloy. As illustrated in Figure 3 [11,12], fixed factors applied in this process are shown in Table 1.

Figure-3. Plasma formation during the plasma-sputtering process.

Table-1. plasma-sputtering parameters.

Fixed parameter	values
Gas used	Ar + O
Total pressure	3.5×10^{-2} mbar
DC voltage	2.5 KV
Discharge current	3 mA

The furnace with inert argon gas was used to recrystallize the niobium oxide deposited on the surface of the titanium sample at 700°C for one hour, and the samples were slowly cooled in the furnace [13,14].

2.3 Characterization of Titanium Alloy

A Scanning-electron-microscope (SEM) LEITS-type was used to identify the surface morphology of the sputtering layer, and its homogeneity with the substrate alloy. X-ray diffraction (XRD) Shimadzu XRD-6000 was utilized to identify phase changes during the alloy modification, using a Ni filter with a Cu target (Kα= 0.15418 nm).

Potentiodynamic polarization was used to determine the general corrosion of the alloy by measuring current density and corrosion potential, while cyclic-potentiodynamic-polarization was utilized to recognize the pitting behavior of this alloy.

This test was conducted in an electrolyte solution similar to body fluid (Ringer solution) at 37°C. It was done at 0.4 mV/s, using an initial potential of 2000 mV above - below open circuit potential to investigate all corrosion behavior,[15].

Table-2. Chemical composition of Ringer solution (100ml), [16].

Elements	Composition (g)
$CaCl_2.2H_2O$	0.033
KCl	0.03
NaCl	0.86
H_2O	qs

The wear test (pin-on-disk) using a pin consisting of a silicon carbide ball with a diameter of 16 mm to determine the wear rates and coefficient of friction. This test was done by applying a normal load of 10N and 15N respectively, a speed 200 rpm (0.2 m/s), sliding distance of 99 m, with a Ringer's solution as the lubricated solution at 25°C. ASTM G99-04 standards were used as a reference in this test.

3. Results and discussions

3.1 Microstructure Observation

The surface morphology and cross-section of modified Ti-6Al-4V alloy by plasma sputtering were evaluated using scanning-electron-microscopy (SEM) as showed in figure 4. The results showed an excellent adhesion between the uniformly thick sputtering layer and the substrate without any detectable gap. Another result identified from SEM was the thickness of the sputtering layer, where the 3 hours sputtering have a thinner layer (4.04 µm) compared to 6 hours sputtering (9.95 µm). The thickness was measured using ImageJ 1.54software. The surface of the alloy after the sputtering process consisted of three regions the first one sputtering layer, the second one heat-affected zone, and the substrate alloy, [17].

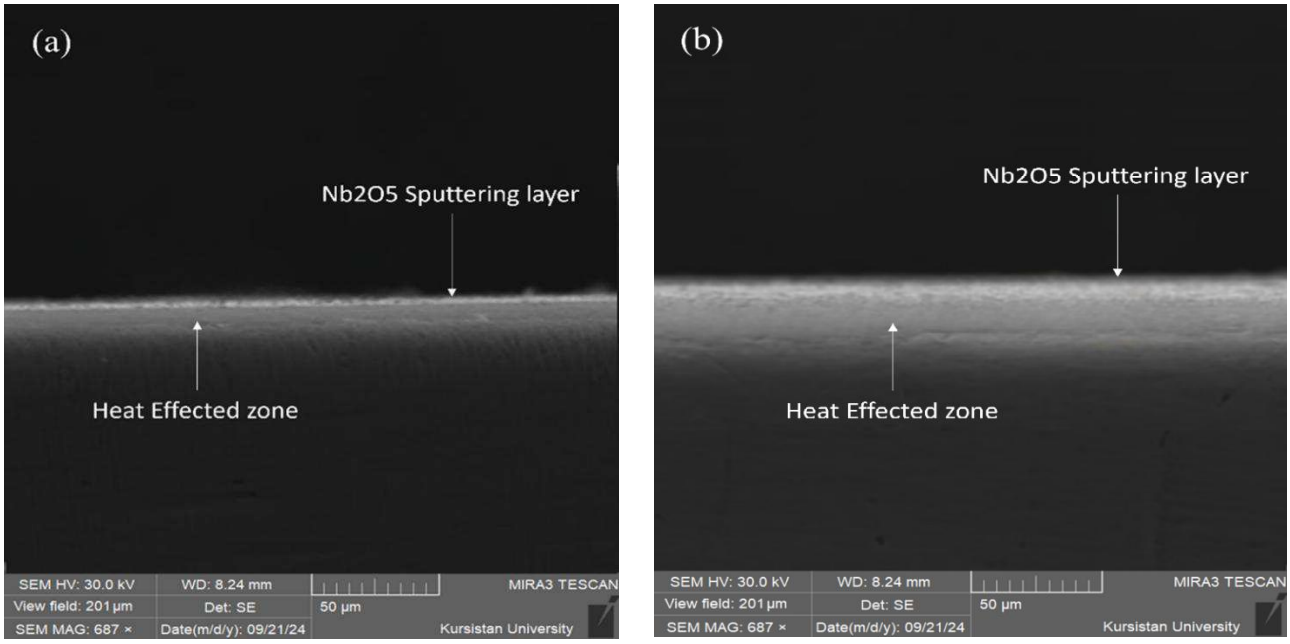

Figure-4. The cross-section area of Ti-6Al-4V alloy for: a- 3-hour plasma reactive sputtering, and; b- 6-hour plasma reactive sputtering.

The results obtained from EDS show significant influence of plasma-sputtering on the chemical composition of Ti-6Al-4V alloy and the sputtering time also has a great influence. where the formation of Nb_2O_5 increases with the time of sputtering and which significantly effects on the wear rate and corrosion resistance. To clarify, the chemical composition was measured at the surface of the specimen as illustrated in Figure 5 and Figure 6.

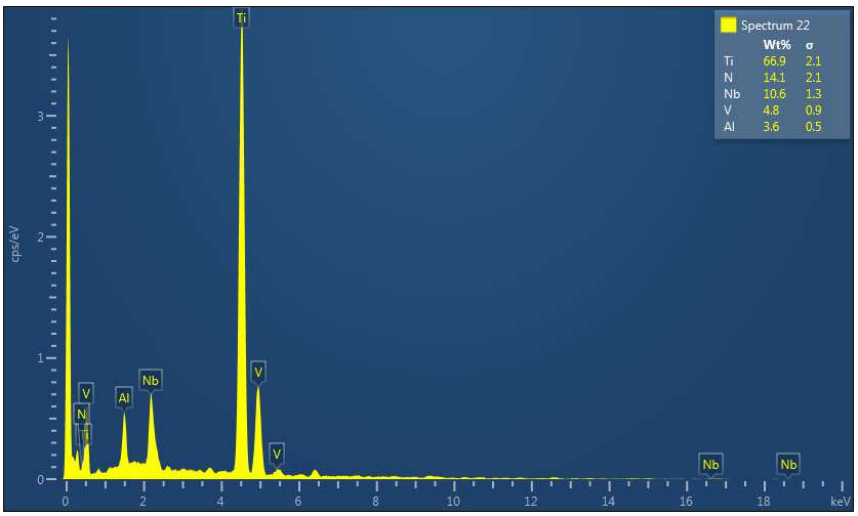

Figure-5. EDX for Ti-6Al-4V alloy for 3-hour plasma reactive sputtering.

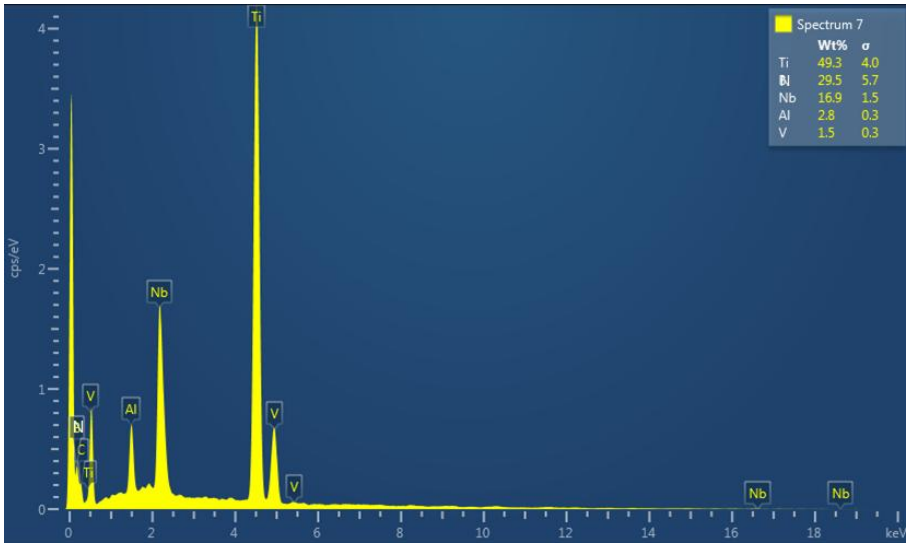

Figure-6. EDX for Ti-6Al-4V alloy for 6-hour plasma reactive sputtering.

3.2 Phase Identification of sputtering alloy

X-ray diffraction (XRD) was employed to identify the phases present. The results shows that the phases present in the untreated sample exclusively α-Ti and β-Ti phases where the diffraction peaks of α-Ti appear at 2θ angles of 35.3°,40.5°, and 63°.while the diffraction peak of β-Ti appears in 2θ angle 38.09° as illustrated in figure 7.

The phase identification after reactive plasma sputtering shows the creation of Nb_2O_5 on the surface of the Ti-6Al-4V alloy. The analysis revealed the phase of Nb_2O_5 present at 3-houer sputtering has a lower peak intensity compared with 6-houer sputtering. Furthermore, the diffraction peaks of Nb_2O_5 are observed at 2θ angles of (22.5°,26.5°,36.8°,39.4°, and 46°). In addition, a slight reduction in the diffraction peaks of α-Ti and β-Ti is observed due to the formation of a thin Nb_2O_5 layer.

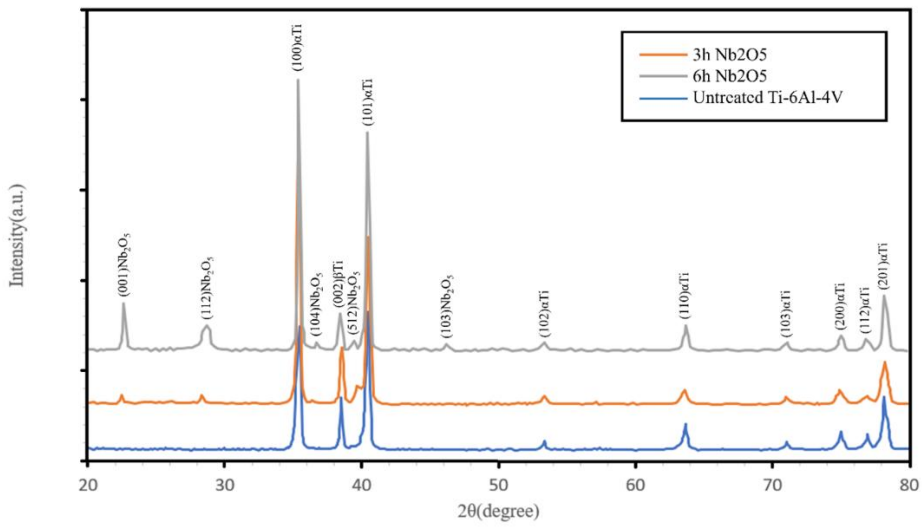

Figure-7. X-ray diffraction of Ti-6Al-4V alloy before and after plasma spluttering**.**

3.3 Corrosion Performance of Plasma Sputtered Ti-6Al-4V Alloy

3.3.1 Tafel potential polarization

The study focuses on the current density and its effect on plasma sputtering time to identify electrochemical behavior of the alloy after and before the treatment immersed in ringer solution at 37ºC as showed in figure 8. This test was conducted using Ringer's solution as an electrolyte at 37°C. As shown from the results, the corrosion current density has an inverse relationship with sputtering time where the minimum current density is observed at 6-hour [18]. In contrast, the base alloy exhibits better corrosion behavior than 3-hour sputtering due to the presence of porosity and amorphous Nb_2O_5 on the surface of Ti-6Al-4V,as shown in the SEM image in Figure 9, These findings are consistent with [19].

Table-3. Corrosion rate for sputtering and untreated Ti-6Al-4V alloy.

(α+β) Ti-6Al-4V alloy	Ecorr (mV)	Icorr *10^{-3} (mA/cm2)	Corrosion Rate (mpy)
3 hours sputtering	-819.3	1.96	6.67×10^{-4}
6 hours sputtering	-172	0.083	0.282×10^{-4}
Untreated	-72.2	0.976	3.343×10^{-4}

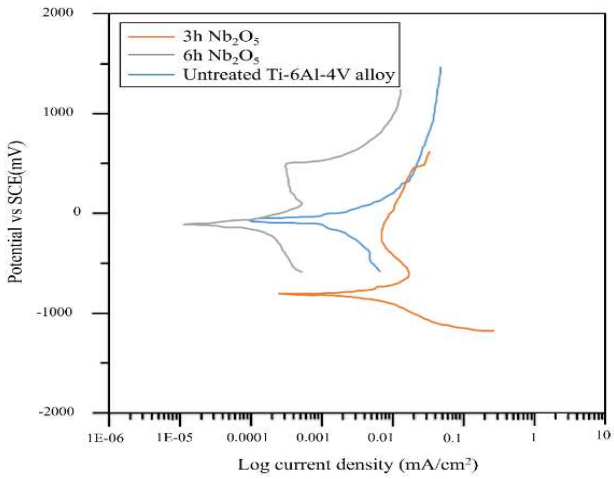

Figure-8. Potentiodynamic polarization curves for Ti-6Al-4V alloy in Ringer solution at 37ºC.

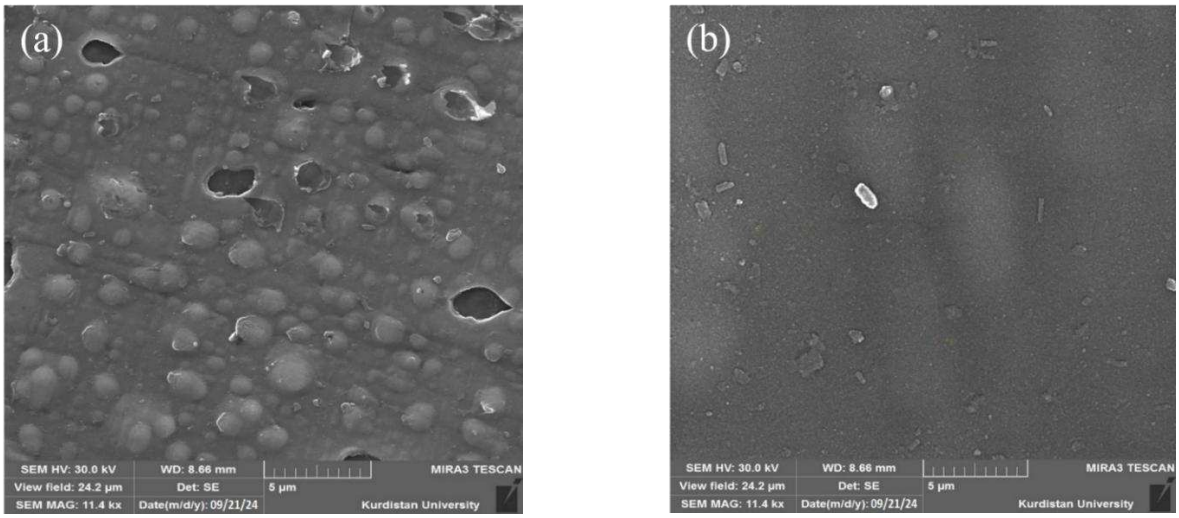

Figure-9. The surface morphology of Ti-6Al-4V alloy for (a) 3-hour plasma reactive sputtering, (b) 6-hour plasma reactive sputtering.

3.3.2 Cyclic Polarization

Concurrently, localized corrosion may occur in aggressive media causing a breakdown of the passive protective film in a specific position leading to the pit formation on the alloy surface. Thus, the resistance of materials to this type of corrosion should be examined, depending on this explanation, this test was conducted by anodic cyclic polarization, [20].

As illustrated in Figure 10 this alloy exhibits a high resistance to pitting corrosion in Ringer's solution at 37ºC in both untreated and reactive sputtered samples. Nonetheless, the passivity increases of alloy with sputtering time.

Table-4. Cyclic polarization parameters in Ringer solution for untreated and reactive sputtering specimens.

Ti-6Al-4V	E Protection (mV)	Passive current density at 500mV (mA/cm^2) cyclic	Passive current density at 500mV (mA/cm^2) tafel
3 hours sputtering	-100	0.0208	0.0283
6hours sputtering	10	0.00011	0.00028
Untreated	-20	0.0101	0.0214

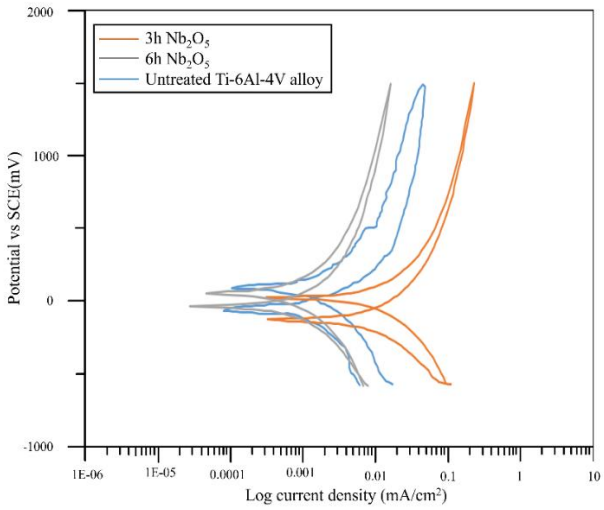

Figure-10. Cyclic polarization curves in Ringer solution for untreated and reactive sputtering specimens.

3.4 Wear Test (Pin on Desk)

Wear rate and friction coefficient play a meager factor in biocompatibility, especially in surgical implants. Therefore, this study investigates the effect of sputtering time on wear performance. Depending on the experimental outcomes, the sputtering time greatly impacts wear rate and friction coefficient. Observably, both wear rate and friction coefficient decrease with increasing sputtering time as a result of the formation of the thin protective layer, as described in previous studies, [21].

Tabel-5. Friction coefficient and Wear rate at room temperature in Ringer solution

Samples conditions	Friction coefficient	Wear rate 10^{-4} (mm^3/Nm)	Load (N)	Sliding speed (rpm)	Time (s)
Untreated	0.46	2.053	10	200	900
3 hours sputtering	0.42	1.824			
6 hours sputtering	0.4	0.684			
Untreated	0.42	2.432	15		
3 hours sputtering	0.38	1.976			
6 hours sputtering	0.32	1.520			

4. Conclusions

Depending on experimental investigation, sputtering time has a significant influence on the thickness of the deposited layer. According to these results:

1- Niobium oxide formation on the surface of Ti-6Al-4V alloy can be revealed through XRD analysis.

2- Scanning electron microscope investigation proves an increase in the thickness of Nb_2O_5 with increasing sputtering time and decreased porosity.

3- The corrosion behavior and wear performance for Ti-6Al-4V alloy will be improved for 6 hours of sputtering time, in contrast to the 3 hours of sputtering time, a decrease in corrosion resistance was observed.

References

[1] Pejakovic V., Totolin V., and Rodriguez M. 2018. Tribocorrosion behaviour of Ti6Al4V in artificial seawater at low contact pressures. Tribology International journal. 119: 55-65.

[2] Guo Y., Zhang B., Zhou L., and Li J. 2025. Creep strain and stress state-dependent creep asymmetry during early-stage room-temperature creep in a titanium alloy. Journal of Materials Science & Technology. 243: 1-14.

[3] Totolin V., Pejaković V., Csanyi T., Hekele O. et al. 2025. Surface engineering of Ti6Al4V surfaces for enhanced tribocorrosion performance in artificial seawater. Materials and Design. 243: 1-14.

[4] Perez N., Alvarez-Vera M., Ortega J. A. et al. 2025. Tribological and microstructural characterization of laser microtextured Ti-6Al-4V ELI alloy evaluated against UHMWPE and PEEK for biomedical applications. Wear. 104: 205931.

[5] Wei G., Tan M., and Attarilar S. 2023. An overview of surface modification, A way toward fabrication of nascent biomedical Tie6Ale4V alloys. Journal of Materials Research and Technology. 24: 5896-5921.

[6] Aghajani H., and Behrangi S. 2017. Plasma nitriding of steels. Springer.

[7] Li J., Zhang Y., and Zhao Y. 2017. Mechanical properties of TiN ceramic coating on a heat treated Ti-13Zr-13Nb alloy. Journal of Alloys and Compounds. 724: 34-44.

[8] Garg R., Gonuguntla S., Sk S. et al. 2024. Sputtering thin films: Materials, applications, challenges and future directions. Advances in Colloid and Interface Science. 330: 103203.

[9] Nguyen H. D., Pramanik A., Basak A. K. et al. 2022. A critical review on additive manufacturing of Ti-6Al-4V alloy: microstructure and mechanical properties. Journal of Materials Research and Technology. 18: 4641-4661.

[10] Qayyum A., Imran M., Khan M. et al. 2024. Spectroscopic evaluation of nitrogen glow discharge for the surface nitriding of Ti-6Al-4V alloy. Surfaces and Interfaces. 44: 103806.

[11] Li H., Ding Y., Hu X. et al. 2024. A comparative study of TiO2, Ta2O5 and Nb2O5 coated Ti6Al4V titanium alloy for biomedical applications. Ceramics International. 50(23, Part B): 50444-50453.

[12] Jilani A., Abdel-wahab M. S., and Hammad A. H. 2017. Advance Deposition Techniques for Thin Film and Coating. Modern technologies for creating the thin-film systems and coatings.

[13] Lertlop W., Sangwaranatee N., Horprathum M., and Kaewkhao J. 2016. Influence of Post-Deposition Annealing on Structure and Optical Characteristics of Niobium Oxide Thin Films. Key Engineering Materials. 675-676: 245-248.

[14] Ma J., Guo X., Xue H. et al. 2020. Niobium/tantalum-based materials: Synthesis and applications in electrochemical energy storage. Chemical Engineering Journal. 380: 122428.

[15] Hsu R. W., Yang C. C., Huang C. A., and Chen Y. S. 2004. Investigation on the corrosion behavior of Ti–6Al–4V implant alloy by electrochemical techniques. Materials Chemistry and Physics. 86(2–3): 269-278.

[16] Ferreira D. F., Almeida S. M. A., Soares R. B. et al. 2019. Synergism between mechanical wear and corrosion on tribocorrosion of a titanium alloy in a Ringer solution. Journal of Materials Research and Technology. 8(2): 1593-1600.

[17] Jin J., Duan H., and Li X. 2017. The influence of plasma nitriding on microstructure and properties of CrN and CrNiN coatings on Ti6Al4V by magnetron sputtering. Vacuum. 136: 112-120.

[18] Jiang J., Wang Q., Huang H. et al. 2014. Microstructure and property changes induced by substrate rotation in titanium/silicon dual-doped a-C:H films deposited by mid-frequency magnetron sputtering. Surface and Coatings Technology. 240: 419-424.

[19] Aygun G., Yildiz I. 2009. Interfacial and structural properties of sputtered HfO2 layers. Journal of Applied physics. 106.

[20] Rybkina A., Gladkikh N., Marshakov A. et al. 2020. Effect of Sign-Alternating Cyclic Polarisation and Hydrogen Uptake on the Localised Corrosion of X70 Pipeline Steel in Near-Neutral Solutions. Metals. 10(2): 245.

[21] Oliveira M., Auricchio V., Ribeiro K. et al. 2024. Enhancing the Wear Performance of 316L Stainless Steel with Nb2O5 Coatings Deposited via DC Sputtering at Room Temperature under Varied Environmental Conditions. Lubricants. 12(10): 345.

Supplementary Files

This is a list of supplementary files associated with this preprint. Click to download.

- tables.docx